WILEY

Connectivity of post-fire runoff and sediment from nested hillslopes and watersheds

Codie Wilson[1] | Stephanie K. Kampf[2] | Sandra Ryan[3] | Tim Covino[2] | Lee H. MacDonald[1] | Hunter Gleason[4]

[1]Natural Resource Ecology Lab, Colorado State University, Fort Collins, Colorado

[2]Department of Ecosystem Science and Sustainability, Colorado State University, Fort Collins, Colorado

[3]Rocky Mountain Research Station, Fort Collins, Colorado

[4]Department of Chemistry, Environmental Science and Environmental Engineering, University of Northern British Columbia, Prince George, Canada

Correspondence
Codie Wilson, Natural Resource Ecology Lab, Colorado State University, Fort Collins, CO.
Email: codie.wilson@colostate.edu

Abstract

Wildfire increases the potential connectivity of runoff and sediment throughout watersheds due to greater bare soil, runoff and erosion as compared to pre-fire conditions. This research examines the connectivity of post-fire runoff and sediment from hillslopes (<1.5 ha; $n = 31$) and catchments (<1000 ha; $n = 10$) within two watersheds (<1500 ha) burned by the 2012 High Park Fire in northcentral Colorado, USA. Our objectives were to: (1) identify sources and quantify magnitudes of post-fire runoff and erosion at nested hillslopes and watersheds for two rain storms with varied duration, intensity and antecedent precipitation; and (2) assess the factors affecting the magnitude and connectivity of runoff and sediment across spatial scales for these two rain storms. The two summer storms that are the focus of this research occurred during the third summer after burning. The first storm had low intensity rainfall over 11 hours (return interval <1–2 years), whereas the second event had high intensity rainfall over 1 hour (return interval <1–10 years). The lower intensity storm was preceded by high antecedent rainfall and led to low hillslope sediment yields and channel incision at most locations, whereas the high intensity storm led to infiltration-excess overland flow, high sediment yields, in-stream sediment deposition and channel substrate fining. For both storms, hillslope-to-stream sediment delivery ratios and area-normalised cross-sectional channel change increased with the percent of catchment that burned at high severity. For the high intensity storm, hillslope-to-stream sediment delivery ratios decreased with unconfined channel length (%). The findings quantify post-fire connectivity and sediment delivery from hillslopes and streams, and highlight how different types of storms can cause varying magnitues and spatial patterns of sediment transport and deposition from hillslopes through stream channel networks.

KEYWORDS

antecedent precipitation, connectivity, nested monitoring, post-fire runoff and erosion, rainfall intensity

1 | INTRODUCTION

Wildfire increases the potential for connectivity of water and sediment across a landscape. Burning combusts organic surface cover creating interconnected areas of bare soil; subsequent rainfall can lead to soil sealing (Larsen et al., 2009) and increased runoff and erosion (Benavides-Solorio & MacDonald, 2005; Ortíz-Rodríquez et al., 2019; Wagenbrenner & Robichaud, 2014). Connectivity typically increases

after fire because post-fire runoff and sediment transport can develop with less rainfall (Wilson et al., 2018) and over smaller drainage areas (Wohl, 2013) than in unburned conditions. Post-fire connectivity is affected by many factors, including topography, burn severity and rainfall (Heckman et al., 2018; Lexartza-Artza & Wainwright, 2009; Wainwright et al., 2011). Complex interactions between these variables determine where and when connectivity occurs; for example, sediment delivered from hillslopes to streams can be stored in-channel for centuries (Moody & Martin, 2001a) or remobilised during subsequent rainfall-runoff events (Duvert et al., 2011).

In many regions, post-fire hillslope responses are produced by infiltration-excess overland flow during spatially variable convective rain storms (Moody et al., 2013; Moody & Martin, 2001a, 2001b). During these storms, the highest rainfall intensities are often concentrated over small areas <10 km^2 (Osborn & Laursen, 1973), leading to spatially variable rates of overland flow and erosion. Areas with high intensity rainfall experience increased peak streamflow and sediment transport within channels (Moody & Martin, 2001a, 2001b), but connectivity of runoff and sediment between hillslopes and channels and along channel networks may be limited to the localised areas affected by high intensity rainfall. Increased erosion often leads to greater sediment storage within channels after a burn, particularly in lower gradient reaches where the frequency of flows capable of sediment transport decreases (Brogan et al., 2019; Moody & Martin, 2001a; Smith et al., 2011). Depending on the sequence of post-fire rain storms, higher overland flow from hillslopes can either erode channel banks and beds where there is a lack of previously stored sediments available for transport or cause aggradation in channels when flow is not high enough to transport all sediment downstream (Brogan et al., 2019; Kampf et al., 2016; Moody & Martin, 2009). Upstream-to-downstream sediment connectivity may be greater for rainfall events with high total depths and following high antecedent rainfall, as these conditions increase runoff and sediment transport capacity of streams (Moody & Martin, 2001a, 2001b; Murphy et al., 2018; Wilson et al., 2018).

Runoff generation and sediment production after wildfire generally decrease over time as burned hillslopes are revegetated. Post-fire mulch treatments can also increase surface cover and associated rainfall interception and storage of runoff and sediment on the ground surface (Wagenbrenner et al., 2006; Robichaud, Jordan, et al., 2013; Robichaud, Wagenbrenner, et al., 2013; Moreno-de Las Heras et al., 2010; Parsons et al., 2006). By three to four years post-fire, typically only the most extreme rainfall events produce a response in overland flow and hillslope erosion (Ebel & Martin, 2017; Moody & Martin, 2001a; Wagenbrenner et al., 2015; Wilson et al., 2018). By four years post-fire, the drainage areas required for channelised flow increase, comparable to unburned conditions (Wohl & Scott, 2017).

Though post-fire responses are well-documented for plot, hillslope, or watershed scales independently, studies linking these scales are needed (Smith et al., 2011). Post-fire runoff and sedimentation create difficulties for emergency management and water treatment (Emelko et al., 2011; Hohner et al., 2016; Martin, 2016), and water supplies depend on forested areas vulnerable to wildfire (Brown et al., 2008; Robinne et al., 2018; Westerling et al., 2006). Concurrent information on the connectivity of runoff and sediment from hillslopes through watershed channel networks can further our understanding of how much sediment will reach water supply intakes and inform potential management decisions (Lexartza-Artza & Wainwright, 2009). In this study we used nested hillslope and stream channel observations post-fire to: (1) identify sources and quantify magnitudes of runoff and sediment transport during two contrasting rain storms that produced substantially different responses: one long duration with low intensity rainfall (<1–2 year return interval) and one short duration event with higher intensity rainfall (<1–10 year return interval); and (2) determine the factors affecting the magnitude and connectivity of runoff and sediment from hillslopes to channels and along channel networks for these storms.

2 | METHODS

2.1 | Site description

In June 2012 the High Park Fire burned 330 km^2 of Colorado Front Range forest draining into the Cache la Poudre and Big Thompson Rivers, with approximately 50% burned at moderate or high severity (BAER, 2012). These watersheds supply drinking water to the cities of Fort Collins, Greeley, Loveland, and other municipalities, so mulch treatments were applied to reduce erosion and sedimentation of water supplies. Areas targeted to receive mulch were those with moderate to high burn severity and steep slopes (BAER, 2012; Figure 1).

Geology of the High Park Fire area is Precambrian metasedimentary and metaigneous schists, gneisses and plutonic igneous rocks (Abbott, 1970). Soils are predominantly sandy loam (BAER, 2012) with moderately high to high saturated hydraulic conductivity and drainage classes ranging from well drained to somewhat excessively drained (Sheriff et al., 2016; Soil Survey Staff, 2019). The primary pre-fire vegetation was ponderosa pine (*Pinus ponderosa*) at lower elevations and denser mixed conifer forests at higher elevations, with grasses and shrubs on drier south-facing slopes (BAER, 2012; Schmeer et al., 2018).

Peak annual streamflow in the Colorado Front Range is rainfall dominated below 2000 m and snowmelt dominated above 3100 m, with mixed sources in-between (Kampf & Lefsky, 2015). Our study sites in the Skin and Hill Gulch watersheds (Figure 1) fall primarily in the mixed streamflow regime, with elevations ranging from 1740–2678 m. Hillslope runoff during our sampling season of June through September is primarily caused by infiltration-excess overland flow driven by convective rain storms. From 2013 to 2015 the average sampling season rainfall was 273 mm. Streams in these watersheds have a small snowmelt runoff peak (e.g., 58–82 L s^{-1} km^{-2} for the outlets of Skin and Hill Gulch in 2015, respectively), and prior to the fire they did not retain streamflow throughout the year. Since the fire, these streams have had perennial flow, with baseflow sustained throughout the summer and fall and brief stormflow responses to summer rains.

2.2 | Monitoring overview

The study was conducted within two watersheds burned by the High Park Fire, Skin and Hill Gulch (15.1 and 14.1 km², respectively; Figure 1). In the months after the fire 29 hillslope sediment fences were installed to measure erosion along with eight co-located tipping bucket rain gauges. In summer 2014 two additional sediment fences and one additional rain gauge were installed within the headwaters of Skin Gulch. These two new sediment fences and two existing sediment fences in the headwaters of Hill Gulch were instrumented to continuously monitor runoff and the amount of sediment that overtopped the sediment fence (Figures 1 and 2; Wilson et al., 2020).
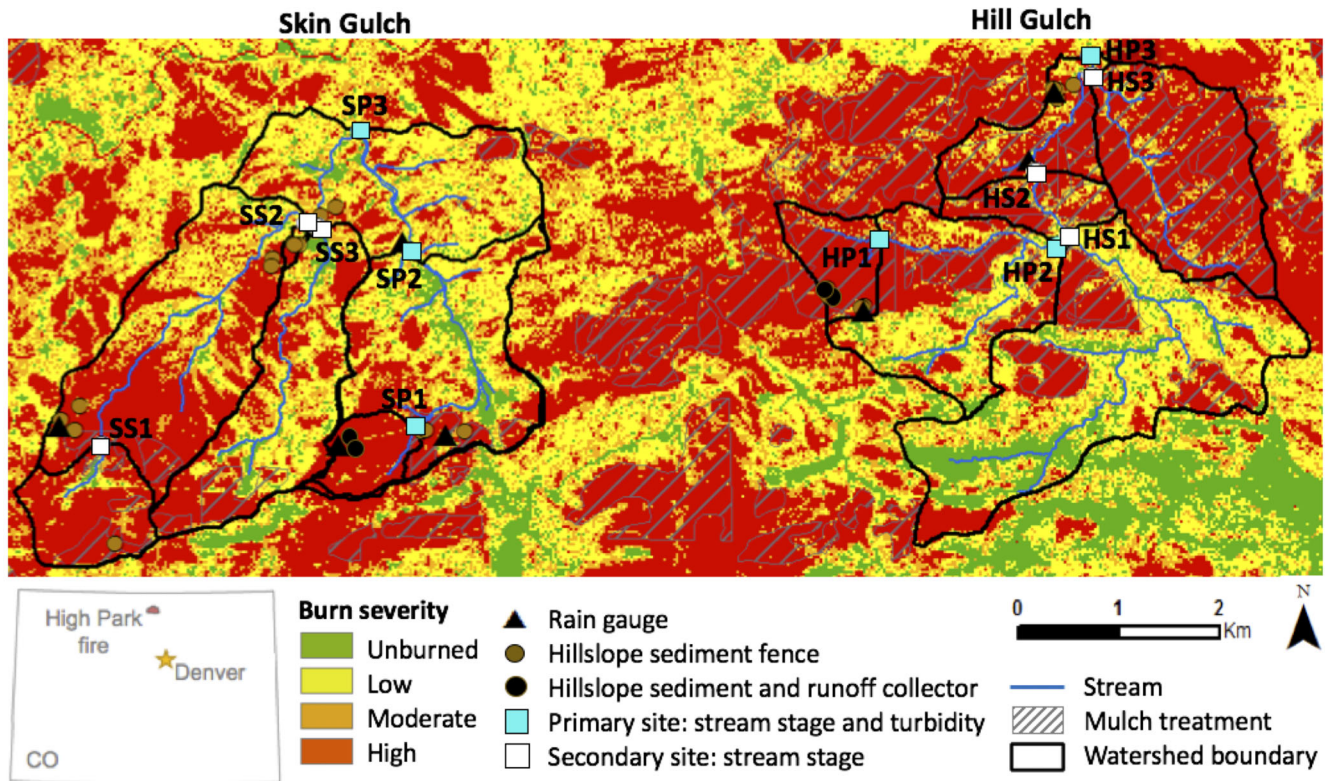
FIGURE 1 Monitoring site locations within Skin and Hill Gulch of the 2012 High Park Fire with burn severity (Stone, 2015), streams, monitoring equipment (i.e., rain gauges, hillslope sediment and/or runoff collectors, stream stage and/or turbidity), areas targeted to receive mulch treatments, and watershed boundaries. Site names correspond to those in Table 1
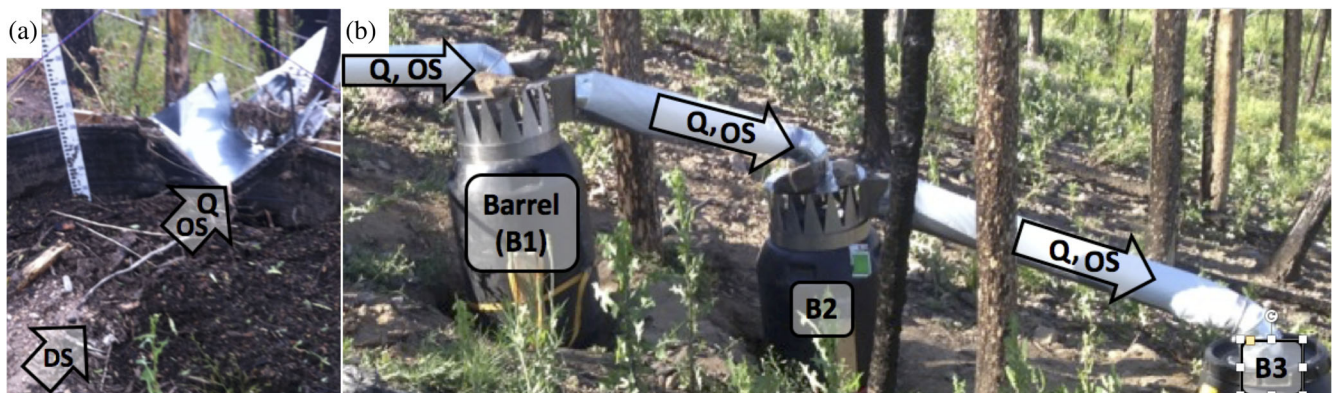
FIGURE 2 The four hillslope sediment fences modified to measure the runoff and sediment overtopping the fence included: (a) sediment fence as shown in the foreground to capture the sediment deposited behind the fence (deposited sediment or DS), a 90° V-notch weir to route the runoff (Q) and suspended sediment that overtopped the fence (overtopped sediment or OS) into a series of three collection barrels, and a staff gauge which was repeatedly photographed with a time lapse camera (upslope; not pictured) to determine the height of water above the weir at 1-min intervals; and (b) side view of the Q and OS collection system with sample collection barrels labelled sequentially as B1, B2, and B3

Contributing areas for the 31 hillslope monitoring sites ranged from 0.1 to 2.8 ha ($\bar{x}$ = 0.5 ha) with average slope of 5–33°, and elevations from 1780–2670 m.

In 2014, the outlets of Skin and Hill Gulch were instrumented to measure stream stage, turbidity, and suspended sediment; three additional nested catchments per watershed (0.6–3.9 km²) were also instrumented to measure stream stage (Figure 1 and Table 1). In 2015, two additional catchments per watershed (1.2–10.0 km²) were added to measure stream stage, turbidity, and suspended sediment; installation was completed by June 23, 2015. Stage height and turbidity were continuously recorded at 1–10 min intervals. Sites with turbidity and suspended sediment monitoring are hereafter referred to as primary sites, while sites where only stage height was monitored are referred to as secondary sites. We focus our analysis on rainfall events during the 2015 sampling season.

2.3 | Precipitation

Rainfall was continuously monitored with three Rainwise tipping bucket rain gauges (resolution of 0.25 mm) in Hill Gulch and five in Skin Gulch (Figure 1). Rainfall data were processed using the USDA Rainfall Intensity Summarisation Tool (USDA-ARS, 2019); storms were separated by at least 6 hours with <1 mm of rain (Renard et al., 1997), and the following metrics were calculated for each event: depth (P; mm); duration (h); maximum intensity (mm h^{-1}) over 5-, 15-, 30-, and 60-minute intervals (MI_5, MI_{15}, MI_{30} and MI_{60}, respectively); and 30-minute erosivity (EI_{30}), where EI_{30} is the product of event rainfall kinetic energy and intensity (MJ mm ha^{-1} h^{-1}; Brown and Foster, 1987). The depth of rainfall (mm) exceeding MI_5 thresholds of 10, 15 and 20 mm h^{-1} was also calculated ($P > 10$, $P > 15$ and $P > 20$, respectively) (Kampf et al., 2016). The daily antecedent precipitation index (I_a) was calculated for each rain gauge across the sampling season as:

$$I_a = I_o k + I \qquad (1)$$

where I_o is the initial value of I_a (mm), k is the recession factor set to 0.9, and I is the rainfall (mm) for a given day (Dingman, 2002). To help characterise the initial conditions affecting site responses to rain events, differences in I_a between events were determined using t-tests with a significance level of 0.05.

Five telemetered USGS rain gauges in the vicinity of Skin and Hill Gulch (https://co.water.usgs.gov/infodata/COPrecip/index.html) were monitored to determine when sufficient rainfall occurred to warrant visit sites for the collection of runoff and sediment. Site visits were conducted 1–19 days after rain storms. When multiple storms occurred between site visits, the primary causal storm for each site with continuous monitoring was determined as that coinciding with the largest recorded runoff and turbidity peak. For hillslope sediment fences the causal storm was assumed to be the one with the highest EI_{30} (Benavides-Solorio & MacDonald, 2005; Wilson et al., 2018).

2.4 | Hillslope runoff and erosion

During each site visit the mass of sediment deposited upslope of each sediment fence was recorded in the field to the closest 0.5 kg using a hanging scale, and a representative sample was collected for analysis

TABLE 1 Characteristics of Skin (S-) and Hill (H-) Gulch primary (-P) and secondary (-S) in-stream monitoring sites including drainage area (km²), elevation range (m), mean watershed and channel slopes (°), percent of watershed burned at high severity, percent of watershed targeted for mulch treatments, and percent of channel length that is unconfined.

Site	Area (km²)	Elevation range (m)	Watershed slope (°)	Channel slope (°)	High burn severity (%)	Mulch (%)[a]	Unconfined channel (%)
SP1	0.6	2429–2486	11	8	97	3	50
SP2	3.9	2180–2485	12	6	41	0	52
SP3	15.1	1889–2678	23	5	44	9	61
SS1	1.2	2449–2678	11	5	79	26	100
SS2	5.2	1984–2593	24	6	44	4	26
SS3	2.8	1970–2642	20	8	41	13	40
HP1	0.8	2049–2377	22	6	89	77	0
HP2	3.6	1867–2392	24	5	53	39	31
HP3	14.1	1741–2224	28	4	51	5	63
HS1	5.7	1858–2379	22	4	28	19	85
HS2	10.0	1821–2392	23	4	40	30	66
HS3	2.9	1751–2229	24	6	83	90	27

Note: Primary sites (SP- and HP-) have streamflow and suspended sediment data, while secondary sites (SS- and HS-) have only streamflow data. Site names correspond to those in Figure 1.
[a]Percentage based on GIS polygons of the areas targeted to receive mulch treatments as in Figure 1.

of gravimetric water content (ASTM D2974-13 Test Method A; ASTM, 2013). The water content was used to adjust the field-wet mass of sediment to a dry mass, which was then normalised by upslope contributing area to obtain an event-based sediment yield in Mg ha^{-1}.

The four sediment fences modified to collect the runoff and sediment that overtopped the fence in addition to the sediment deposited behind the fence each had a 90° V-notch weir that routed runoff and suspended sediment into a series of three 250 L barrels (Figure 2). The first two barrels each had a flow splitter (Bonilla et al., 2006) installed at the top of the barrel that divided the flow into 15 directions, and 1/15 of the flow was transferred to the subsequent barrel(s). To determine stage height (h) above the weir, a time lapse camera photographed the weir and an adjacent staff gauge at 1-min intervals (Figure 2). Hillslope runoff (Q_h) was calculated as (Haan et al., 1994):

$$Q_h = 4.89 * 10^{-8} h^{2.48} * 1000 \qquad (2)$$

where Q_h is in L s^{-1} and h is the height of the water above the weir (mm). The total volume of runoff (L) for each event was divided by contributing area (m^2) to calculate area-normalised runoff (Q; mm), and the runoff ratio (Q/P) was calculated by dividing runoff depth (mm) by the rainfall depth (mm) of the causal storm.

For the four hillslopes with runoff collection systems the amount of sediment that overtopped each sediment fence was determined by stirring the runoff within each barrel and collecting and a 500-ml depth-integrated sample. The sediment concentration (mg L^{-1}) of each sample was determined through wet sieving and filtration (ASTM D3977-97 Test Method C; ASTM, 2013). The overtopped sediment yield (Mg ha^{-1}) was calculated by multiplying the average sediment concentration (mg L^{-1}) by runoff volume (L) and dividing by contributing area. The total sediment yield (Mg ha^{-1}) was the sum of the sediment deposited behind the fence and the overtopped sediment yield.

2.5 | Streamflow and suspended sediment

Stage height was continuously recorded at all 12 in-stream monitoring sites using either capacitance rods (TruTrack WT-HR 1000mm Auckland, NZ) or pressure transducers (Model PDCR 1230 Druck) connected to data loggers (CR1000 or CR10X; Campbell Scientific Inc., Logan, UT). Rating curves were developed to relate streamflow to stage height using the sudden-salt injection method (Kilpatrick & Cobb, 1985) at all sites except for the watershed outlets, where the velocity-area method (Nolan & Shields, 2000) was employed (Section S1.2, Table S1, and Figures S1 and S2). Stormflow was separated from baseflow by drawing a line with a slope of 0.009 L s^{-1} km^{-2} min^{-1} from the initial rise of hydrograph until the falling limb of the hydrograph was intercepted (Hewlett & Hibbert, 1967). Stormflow was used to compute the area-normalised runoff (Q; mm) and runoff ratio (Q/P). Peak flow (L s^{-1} km^{-2}) was also computed and includes baseflow.

Turbidity (NTU) was monitored at each of the three primary monitoring sites in Skin and Hill Gulch using DTS-12 sensors (FTS Inc., Victoria, B.C.) and data loggers (CR1000 or CR10x; Campbell Scientific Inc., Logan, UT). NTU was related to suspended sediment concentrations (SSC; mg L^{-1}) using concurrently collected NTU values and suspended sediment samples. Suspended sediment samples were collected using depth-integrated and siphon samplers (c.f., Mackay & Taylor, 2012) at all primary monitoring sites and automated ISCO samplers at the watershed outlets. Separate rating curves to estimate SSC from the measured NTU values were developed for Skin and Hill Gulch. Due to unusually high SSC samples in Hill Gulch, two NTU-SSC rating curves were developed to represent the "high" (i.e., all samples) and "low" (i.e., SSC <10,000 mg L^{-1}) scenarios (Figure S2 and Table S1). For more detailed information, see supplemental methods (Section S1.3).

Area-normalised in-stream suspended sediment yields (SSY; Mg ha^{-1}) were calculated for each site-event as:

$$SSY = \frac{\sum_{i}^{n}(SSC_i \times Q_i)}{A} \qquad (3)$$

where SSC_i is the suspended sediment concentration (mg L^{-1}), Q_i is the volume of streamflow (L) for the sample interval, and A is the drainage basin area (ha).

To help indicate the possible sources of sediment, SSC was plotted as a function of streamflow during the rising and falling limbs of each event hydrograph. This relationship is often hysteretic, and the direction of the loop from rising to falling limb can be used to infer sources of sediment (Williams, 1989): clockwise loops indicate remobilisation of in-stream sediment because this sediment is readily available, whereas counterclockwise loops indicate the predominance of hillslope inputs because this sediment takes longer to reach a stream (Beel et al., 2011; Duvert et al., 2011; Williams, 1989). Secondary hysteresis patterns for a single storm (e.g., a clockwise loop followed by a counterclockwise loop) indicate multiple sources of sediment.

Sediment delivery ratios (SDRs) were computed as a means of estimating how much of the eroded hillslope or upstream sediment was delivered downstream. Hillslope-to-stream SDRs and upstream-to-downstram SDRs were calculated as the sediment yield (Mg ha^{-1}) at each primary monitoring site divided by, respectively: the sediment yield at each monitored hillslope within the catchment (Walling, 1983); and the sediment yield of each upstream primary monitoring site. SDRs were multiplied by 100 to report values as percentages; higher SDRs indicate more sediment was delivered from a hillslope or upstream monitoring site. Because the monitored hillslopes do not cover the full area contributing to the streams, hillslope-to-stream SDRs should be considered an index of connectivity between hillslopes and channels rather than an accurate quantity.

2.6 | Channel surveys

In-stream surveys were conducted at five channel cross-sections per primary monitoring site before and after rain storms using a Cygnus

2LS Total Station, a handheld Trimble Nomad datalogger and a prism attached to an adjustable wading rod (accuracy of < 5 mm). Cross-sectional area was calculated for each survey using linear interpolation between survey points with the approx function in R Version 3.4.3 (R Core Team, 2017). Cross-sectional areas collected before and after each rain storm were differenced to determine the net and absolute changes in cross-sectional area (m^2). Changes were normalised by catchment area (m^2) to facilitate comparisons across sites. For more detailed information, see supplemental methods (Section S1.4).

2.7 | Geographic analyses

Catchment boundaries and channel networks were delineated in ArcGIS 10.3.1 (ESRI, 2013) using LiDAR imagery with 0.75 m resolution. Channel networks were derived from a flow accumulation grid with a minimum drainage area for channel initiation of 0.2 km^2 as this matched field observations of channelised flow (Martin, 2018). Catchment slope was calculated as the average pixel slope for all cells in a catchment, and channel slope was calculated for 10 m increments and averaged over the length of interest. We calculated the percent of each catchment that burned at high severity from a burn severity map with 25 m resolution (Stone, 2015), and the percent of each catchment targeted to receive mulch treatments (BAER, 2012) (Table 1).

Confined channel reaches with limited floodplains may limit opportunities for storage of runoff and sediment between hillslopes and channels. The Valley Confinement Algorithm (VCA) (Nagel et al., 2014) was used to calculate the percent by length of unconfined stream channels within each catchment. Due to processing time the 0.75 m resolution LiDAR was scaled up to 2 m, and the VCA was

calibrated until the unconfined reaches matched visual field observations.

Correlation analysis was conducted to evaluate the relationships between rainfall, runoff and sediment responses, and site characteristics. Relationships between the following were analysed across all monitoring sites for which the data were available: rainfall event metrics, site attributes (Sections 2.7 and S1.1), and response variables (Sections 2.4–2.6). Data were transformed to natural logarithms to normalise distributions when needed. Analyses used Pearson's correlation coefficients (r) except for hillslopes, for which Spearman's ρ was used because many response variables had values of 0, which limited the utility of Pearson correlation analyses. Our significance level for all analyses was $p \leq 0.05$.

3 | RESULTS

3.1 | Precipitation

The number of rain storms and total rainfall from June through September 2015 was similar in Skin and Hill Gulch, as Skin Gulch had 41 events totalling 140 mm and Hill Gulch had 36 events totalling 160 mm. Between 5–11% of these rain storms generated a response at either a hillslope sediment fence or a primary monitoring site, corresponding to MI_{60} rainfall thresholds of 7–18 mm h^{-1} (Wilson et al., 2018). However, most rain storms did not occur simultaneously in both watersheds, and streamflow responses across all in-stream monitoring sites were only generated on July 8th and August 16th; average MI_{60} rainfall for these storms was 6 and 14 mm h^{-1}, respectively (Table 2). We focus on our analysis on these two storms due to their similar spatial exent and varied rainfall characteristics.

TABLE 2 Rainfall depth (P; mm), maximum 60-minute intensity (MI_{60}; mm h^{-1}), runoff (Q; m), runoff ratio (Q/P), peak streamflow (Peak Q; L s^{-1} km^{-2}) and sediment yield (Mg ha^{-1}) at each in-stream monitoring site for the rain storms on July 8th ("July") and August 16th ("August").

Site	P (mm) July	P (mm) August	MI_{60} (mm h^{-1}) July	MI_{60} (mm h^{-1}) August	Q (mm) July	Q (mm) August	Runoff ratio (Q/P) July	Runoff ratio (Q/P) August	Peak Q (L s^{-1} km^{-2}) July	Peak Q (L s^{-1} km^{-2}) August	Sediment yield (Mg ha^{-1}) July	Sediment yield (Mg ha^{-1}) August
SP1	22	6	5	5	0.01	0.01	0.0002	0.001	8	5	0.0001	0.00001
SP2	19	11	5	12	0.06	0.06	0.003	0.005	21	30	0.0002	0.001
SP3	17	11	5	11	0.12	0.02	0.007	0.002	10	7	0.0002	0.0001
SS1	21	6	6	6	0.06	0.01	0.003	0.002	18	10	—	—
SS2	17	8	6	9	0.09	0.01	0.005	0.002	11	6	—	—
SS3	17	9	5	9	0.19	0.05	0.01	0.005	13	29	—	—
HP1	22	25	6	22	0.36	3.4	0.02	0.1	29	1600	0.003	0.2
HP2	21	23	6	21	0.19	1.1	0.009	0.05	31	1000	0.002	0.01
HP3	20	21	7	19	0.26	4.3	0.01	0.2	13	160	0.001	0.03
HS1	20	20	7	19	0.15	0.2	0.007	0.01	21	30	—	—
HS2	21	21	7	20	0.04	0.05	0.002	0.002	7	39	—	—
HS3	19	19	7	19	0.17	0.4	0.009	0.02	11	160	—	—

Note: Site names correspond to those in Figure 1 and Table 1, and "—" indicates data were not collected at these sites.

## 3.2 | Production and connectivity of runoff and sediment

3.2.1 | July 8th: Long duration, low intensity rainfall

The first storm that generated a runoff and sediment response throughout our monitoring network occurred on July 8, 2015 (Figure 3) with an average of 21 mm of rainfall (range = 16 to 25 mm) over 11 hours (range = 7 to 14 h). Rainfall was recorded at most rain gauges during the preceding 6–9 days, and the rainfall on July 8th represented, on average <34% (range = 156%) of the total rainfall over that time. The return interval of this rainfall event, estimated from two nearby NOAA Atlas stations (Site IDs 05-6925 and 05-3007) was <1 year for durations ranging from 5 min to 3 days (Perica et al., 2013); for rainfall depths over 4–10 days (48–72 mm) the return interval increased to 2 years across gauges in Skin Gulch and at mid- and high-elevation gauges within Hill Gulch (Figure 1). Antecedent precipitation (I_a) averaged 49 mm (range = 20 to 64 mm).

This low intensity rainfall event produced limited overland flow. Hillslope runoff did not overtop the weir at any of the four sediment and runoff collection sites, but sediment was captured at 10 other sediment fences in Skin and Hill Gulch with an average sediment yield of 0.01 Mg ha^{-1}. Sediment yields from eight fences in Skin Gulch ranged from 0.001 to 0.05 Mg ha^{-1}, and yields from two fences in Hill Gulch ranged from 0.01 to 0.02 Mg ha^{-1} (Table 3 and Figure 4). In contrast to the hillslopes, all streamflow monitoring sites responded to this event. Runoff depth averaged 0.2 mm across sites in both Skin and Hill Gulch, with a range of 0.01–0.2 mm in Skin Gulch and a slightly higher range of 0.04–0.4 mm in Hill Gulch; on average, only about 1% of the rainfall became stormflow (Table 2). Peak flow was also similar across both watersheds with an average of 14 L s^{-1} km^{-2} (range = 8 to 21) in Skin and 19 L s^{-1} km^{-2} (range = 7 to 31) in Hill Gulch (Figure 3). In-stream sediment yields differed between Skin and Hill Gulch, with an average of 0.0002 Mg ha^{-1} in Skin (range = 0.0001 to 0.0002) and 0.002 Mg ha^{-1} in Hill Gulch (range = 0.001 to 0.003) (Table 2).

Streamflow and in-stream sediment yields were most strongly correlated to rainfall intensity and watershed slope (Table 4). The quantity of rainfall exceeding a MI$_5$ of 10 mm h^{-1} (P > 10; mm) was positively correlated with Q (mm), Q/P, and in-stream sediment yields for this storm (r^2 = 0.64 to 0.97; Table 4). However, across all sites P > 10 was only 2–4 mm, meaning that the depth of rainfall exceeding the 5-minute intensity threshold of 10 mm h^{-1} was small. Q and Q/P were slightly more correlated with watershed slope (r^2 = 0.68) than with P > 10 (r^2 = 0.67 and 0.64, respectively; Table 4). In-stream sediment
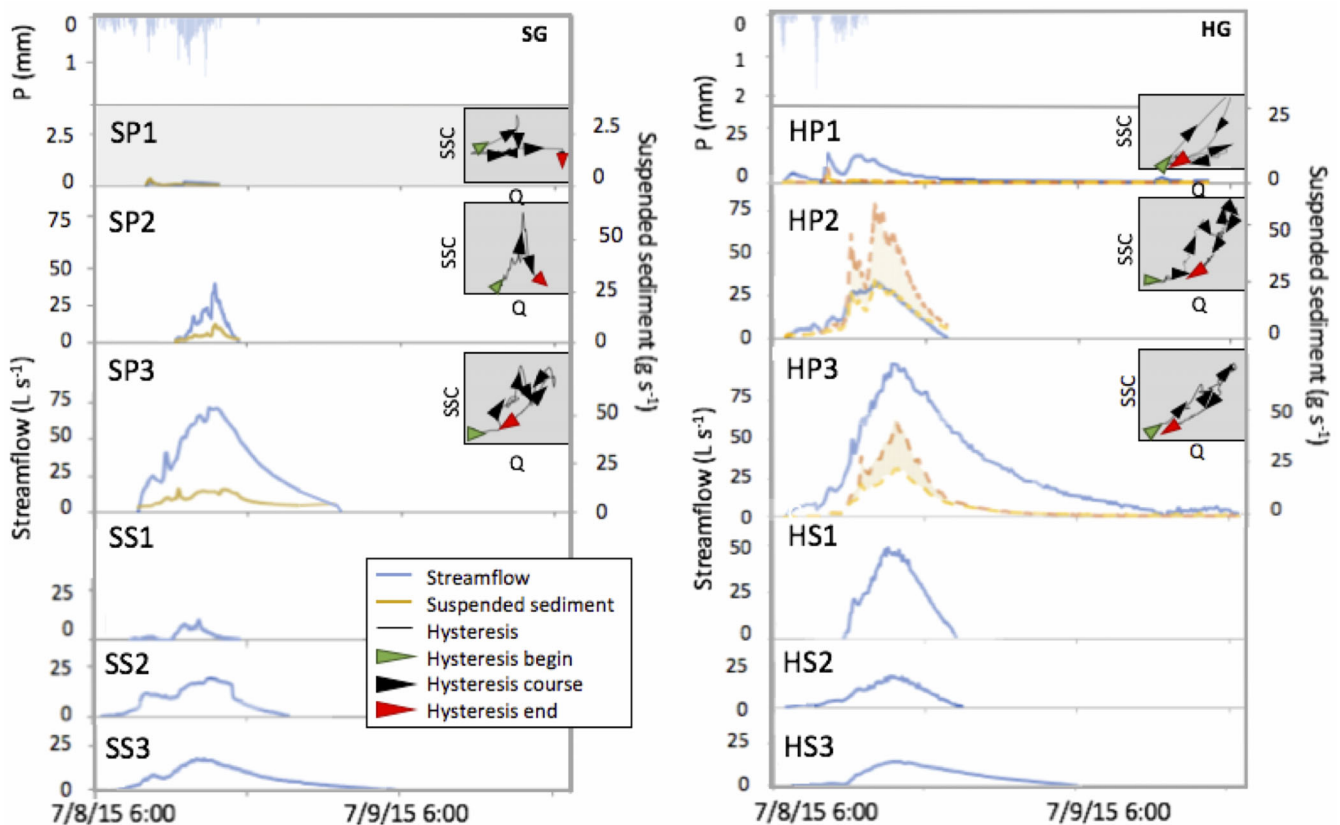
FIGURE 3 Precipitation, streamflow, and in-stream sediment responses for the rain storm on July 8th in Skin (SG; left) and Hill Gulch (HG; right). The top panel shows rainfall depth (P; mm), and subsequent panels show streamflow (Q; L s^{-1}), suspended sediment concentration (SSC; g s^{-1}), and hysteresis patterns (inset; Q vs. SSC) for each site with available data. Site names correspond to those in Figure 1 and Table 1. Upper and lower lines for SSC at Hill Gulch primary monitoring sties (i.e., HP-) represent "high" and "low" rating curve estimates, respectively. The y-axis limits are consistent across sites except for SP1 which is shaded to indicate a much smaller range of values
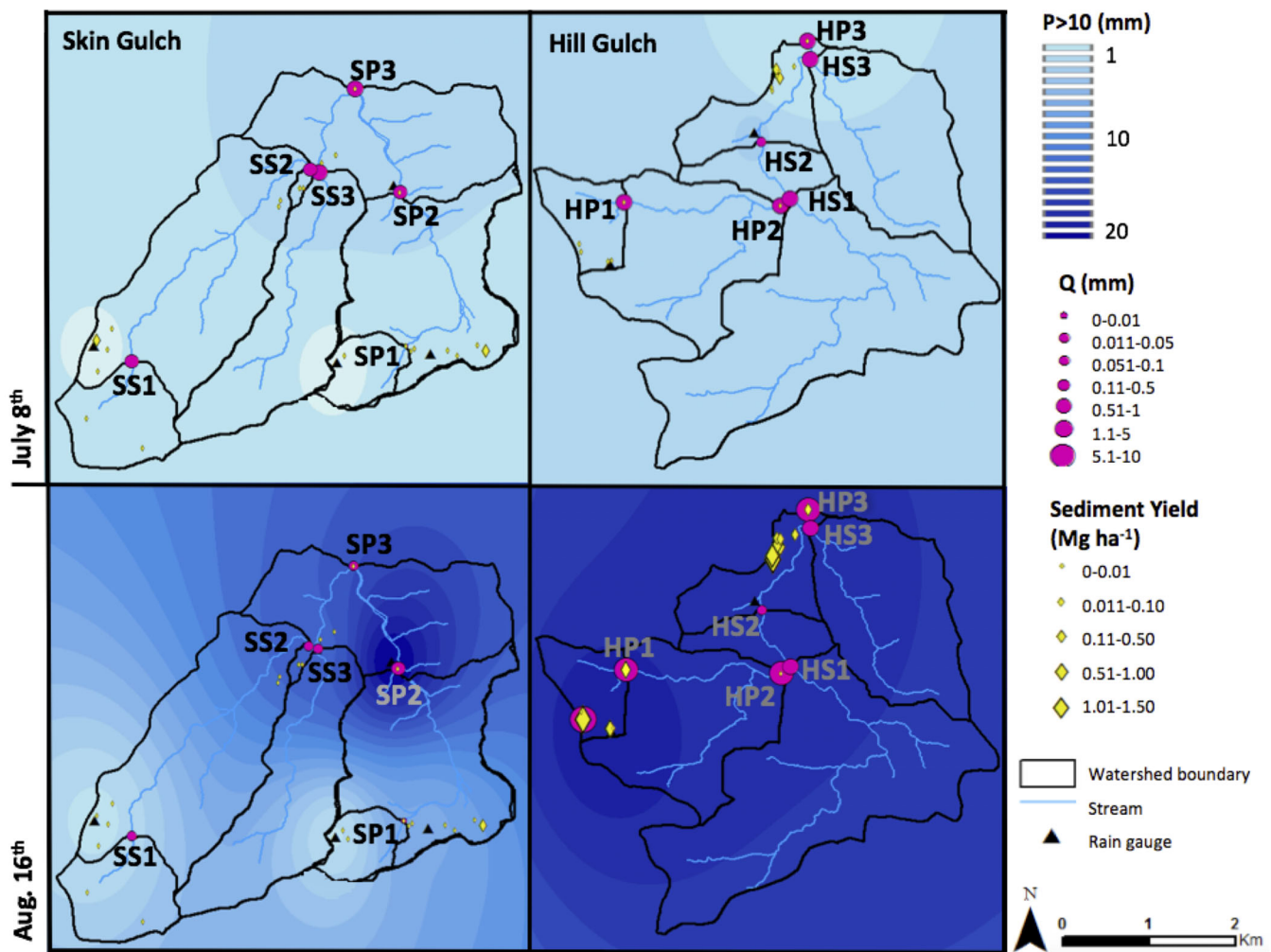
FIGURE 4 Rainfall (P > 10; mm), runoff (Q; mm), and sediment yields (Mg ha^{-1}) within Skin (left) and Hill Gulch (right) for the rain storms on July 8th (upper) and August 16th (lower). The in-stream sediment yields for Hill Gulch were calculated from the "high" rating curve

yields were most correlated to P > 10 (r^2 = 0.97) and slightly less correlated to rainfall erosivity (r^2 = 0.85) and all streamflow metrics (r^2 = 0.83 to 0.85; Table 4). Site responses were likely produced by infiltration-excess overland flow in some parts of the watersheds and possibly seepage from the soil-bedrock interface (Kampf et al., 2016).

The hysteretic SSC vs. streamflow patterns during this event were clockwise, indicating the predominance of in-stream sources of sediment (Williams, 1989) (Figure 3). This is consistent with the limited hillslope runoff and erosion recorded for the event. Secondary hysteresis patterns were also evident at most sites, which may indicate both in-stream and hillslope sources (Figure 3). However, hillslope-to-stream SDRs were low (<1–30%) for both Skin and Hill Gulch, indicating that much of the sediment produced at hillslopes was not delivered to the catchments (Table 3). Hillslope-to-stream SDRs increased with most rainfall (specifically, MI$_{30}$, MI$_{60}$, erosivity and P > 10) and runoff metrics (Q, Q/P) and with the percent of a catchment that burned at high severity (Table 4). Upstream-to-downstream SDRs were higher, at 50–70% in Hill Gulch (Table 3) and 100–200% in Skin Gulch, indicating high connectivity of sediment transport along the channel and additional sediment inputs at downstream locations.

Changes in the cross-sectional areas of channels further support the finding that sediment generated during this event was primarily from in-stream sources. Surveyed cross-sections reveal average net changes of −0.11 m^2 (range = −0.33 to 0.05, Table S4, and Figures S3–S8) indicating the predominance of stream incision. The number of sites with incision throughout Skin and Hill Gulch was similar (67%), but the sum of incision (m^2) and absolute change (m^2) across all cross-sections within Skin were only about half of those observed in Hill Gulch (Table S4) consistent with the slightly higher runoff values recorded in Hill Gulch. Area-normalised absolute change increased with MI$_5$ (r^2 = 0.83) and the percent of a catchment that burned at high severity (r^2 = 0.92; Table 4).

3.2.2 | August 16th: High intensity, short duration rainfall

The second rain storm with responses from hillslope to watershed scale in both watersheds had greater rainfall intensity and peak flow than observed during the July 8th event, with the highest rainfall

TABLE 3 Hillslope sediment yields (SY; Mg ha^{-1}) and hillslope-to-stream sediment delivery ratios (SDR; %) for the July 8th and August 16th rain storms. For in-stream sediment yields refer to Table 2; SP1 is not shown here because none of the associated hillslopes produced measurable sediment during either rain storm.

In-stream site	Hillslope	July 8th SY (Mg ha^{-1})	SDR (%)	August 16th SY (Mg ha^{-1})	SDR (%)
SP2	SP2-a	0.009	2	0	—
	SP2-b	0.003	7	0	—
	SP2-c	0.005	4	0.004	25
	SP2-d	0.02	1	0.08	1
SP3	SP2-a	0.009	2	0	—
	SP2-b	0.003	7	0	—
	SP2-c	0.005	4	0.004	3
	SP2-d	0.02	1	0.08	0.1
	SS1-a	0.05	0.4	0	—
	SS1-b	0.006	3	0	—
	SS1-c	0.003	7	0	—
	SS1-d	0.001	20	0	—
HP1	HP1-a	0	—	0.006	3000
	HP1-b	0	—	0.3	70
	HP1-c	0	—	1.7	10
	HP1-d	0	—	0.007	3000
HP2	HP1-a	0	—	0.006	200
	HP1-b	0	—	0.3	3
	HP1-c	0	—	1.7	1
	HP1-d	0	—	0.007	100
HP3	HP1-a	0	—	0.006	500
	HP1-b	0	—	0.3	10
	HP1-c	0	—	1.7	2
	HP1-d	0	—	0.007	400
	HS3-a	0.02	5	0.4	8
	HS3-b	0	—	0.1	30
	HS3-c	0	—	0.03	100
	HS3-d	0.01	10	0.06	50
	HS3-e	0	—	0.8	4
	HS3-f	0	—	1	3
	HS3-g	0	—	0.01	300

Note: Hillslopes are named for the nearest in-stream monitoring site, and SY is reported as the sediment deposited behind the fence except for HP1-c on August 16th, where SY represents the sum of the deposited and overtopped sediment. "—" indicates SDR was incalculable due division by zero.

intensities and peak flows in Hill Gulch (Table 2 and Figure 4). This event occurred on August 16, 2015 in response to an average of 15 mm (range = 4 to 26) of rainfall over 1 hour (range = 0.4 to 2.3 h; Figure 5). The return interval of this storm was between 5–10 years for maximum rainfall intensities over 5- to 15-minutes (i.e., MI$_5$ and MI$_{15}$) and <1–5 years for longer time intervals (i.e., MI$_{30}$, MI$_{60}$ and 0.5–3 h depths; Perica et al., 2013). In Hill Gulch, MI$_5$ averaged 124 mm h^{-1} (range = 116 to 128), and MI$_{15}$ averaged 71 mm h^{-1} (range = 69 to 72); rainfall intensity in Skin Gulch was slightly lower with average MI$_5$ of 72 mm h^{-1} (range = 22 to 149) and average MI$_{15}$ of 38 mm h^{-1} (range = 14 to 77). The greatest rainfall depths and intensities were measured at the Hill Gulch headwater (HP1) and

intermediate (HP2) primary monitoring sites and near the outlets of the Skin Gulch intermediate (SP2) and outlet (SP3) primary monitoring sites (Figure 4). Antecedent precipitation (I_a) averaged 29 mm (range = <1 to 115), which was significantly lower than the July 8th event.

Runoff and erosion were produced at many hillslopes during the August 16th storm, particularly in Hill Gulch. Sediment was collected at just two out of 20 sediment fences in Skin Gulch with a range of 0.004–0.08 Mg ha^{-1} ($\bar{x}$ = 0.04 Mg ha^{-1}), while all 11 sediment fences in Hill Gulch produced much greater sediment yields of 0.01–1.3 Mg ha^{-1} ($\bar{x}$ = 0.4) (Table 3 and Figure 4). Runoff and sediment overtopped the weir at one of the two hillslope runoff and sediment

TABLE 4 Pearson's correlation coefficients for the July 8th (left) and August 16th (right) rain storms at in-stream monitoring sites between rainfall, catchment and channel characteristics, and runoff (Q; mm), runoff ratio (Q/P), peak flow (peak Q; L s^{-1} km^{-2}), in-stream sediment yield (SY; Mg ha^{-1}, using "high" rating curve estimates for Hill Gulch), hillslope-to-stream sediment delivery ratios (SDR; Table 3), and area-normalised net and absolute channel change.

	July 8th							August 16th						
	Log [Q]	Log [Q/P]	Log [Peak Q]	Log [SY]	Log [SDR]	Net change	Abs. change	Log [Q]	Log [Q/P]	Log [Peak Q]	Log [SY]	Log [SDR]	Net change	Abs. change
P (mm)	−0.33	−0.39	0.25	0.20	0.44	−0.43	0.77	**0.89**	**0.79**	**0.85**	**0.96**	0.33	0.04	0.33
Log[P; h]	−0.02	0.04	−0.25	−0.36	−0.34	−0.03	−0.32	**0.81**	**0.73**	**0.82**	**0.88**	**0.44**	0.20	0.48
Log[M$_5$; mm h^{-1}]	−0.18	−0.20	0.19	0.15	**−0.82**	−0.18	**0.83**	**0.80**	**0.69**	**0.73**	**0.91**	0.20	−0.33	−0.02
Log[MI$_{15}$; mm h^{-1}]	0.19	0.15	0.35	0.72	−0.06	0.20	0.80	**0.81**	**0.70**	**0.75**	**0.93**	0.19	−0.29	0.01
Log[MI$_{30}$; mm h^{-1}]	0.42	0.38	0.18	0.80	**0.81**	0.33	0.14	**0.83**	**0.72**	**0.77**	**0.94**	0.22	−0.26	0.05
Log[MI$_{60}$; mm h^{-1}]	0.48	0.45	0.09	0.62	**0.82**	0.37	−0.28	**0.84**	**0.73**	**0.78**	**0.95**	0.28	−0.21	0.10
Log[Erosivity]	0.46	0.45	0.13	**0.85**	0.55	0.28	0.36	**0.82**	**0.71**	**0.76**	**0.93**	0.29	−0.27	0.04
Log[P > 10; mm]	**0.67**	**0.64**	0.42	**0.97**	**0.79**	0.80	0.04	**0.81**	**0.71**	**0.75**	**0.93**	0.21	−0.30	0.01
Log[P > 15; mm]	−0.30	−0.29	0.09	−0.15	**−0.82**	−0.13	0.46	**0.79**	**0.69**	**0.73**	**0.91**	0.17	−0.34	−0.03
Log[P > 20; mm]	−0.26	−0.27	0.11	0.12	**−0.75**	−0.30	0.80	**0.77**	**0.67**	**0.71**	**0.89**	0.23	−0.35	−0.04
Log[Area; ha]	0.33	0.36	−0.23	0.04	0.30	0.38	**−0.91**	−0.36	−0.38	−0.10	0.07	**−0.55**	**−0.94**	**−0.85**
Log [Watershed slope; °]	**0.68**	**0.68**	0.03	0.75	0.50	0.56	−0.18	0.54	0.48	0.46	0.71	−0.06	−0.33	−0.07
High burn severity (%)	−0.29	−0.33	−0.02	−0.07	**0.79**	−0.51	**0.92**	0.05	0.04	0.17	−0.07	**0.64**	**0.97**	**0.87**
Log[Mulch; %]	0.35	0.33	0.06	0.66	0.27	0.09	0.52	0.44	0.37	0.44	0.46	0.37	0.40	0.56
Log[Mainstem slope; °]	−0.42	−0.39	−0.25	−0.53	**−0.78**	−0.63	0.61	−0.45	−0.42	−0.26	−0.60	0.39	0.73	0.51
Log[Unconfined; %]	−0.17	−0.19	0.03	−0.56	0.44	0.08	−0.43	−0.14	−0.02	−0.30	−0.22	**−0.64**	−0.23	−0.45
Log[Q; mm]		**1.00**	**0.59**	**0.85**	**0.69**	**0.89**	−0.15		**0.96**	**0.91**	**0.98**	0.19	−0.02	0.25
Log[Q/P]			0.56	**0.83**	**0.62**	**0.90**	−0.19			**0.83**	**0.95**	0.17	−0.09	0.19
Log[Peak Q; L s^{-1} km^{-2}]				**0.85**	0.31	0.71	0.20				**0.93**	**0.56**	0.18	0.45
Log[SY; Mg ha^{-1}]					**0.82**	0.67	0.25					0.39	0.03	0.32
Log[SDR]						−0.52	0.24						0.63	0.63
Net change							0.00							0.00

Note: Values in bold italic font significant at *p* ≤ 0.05.
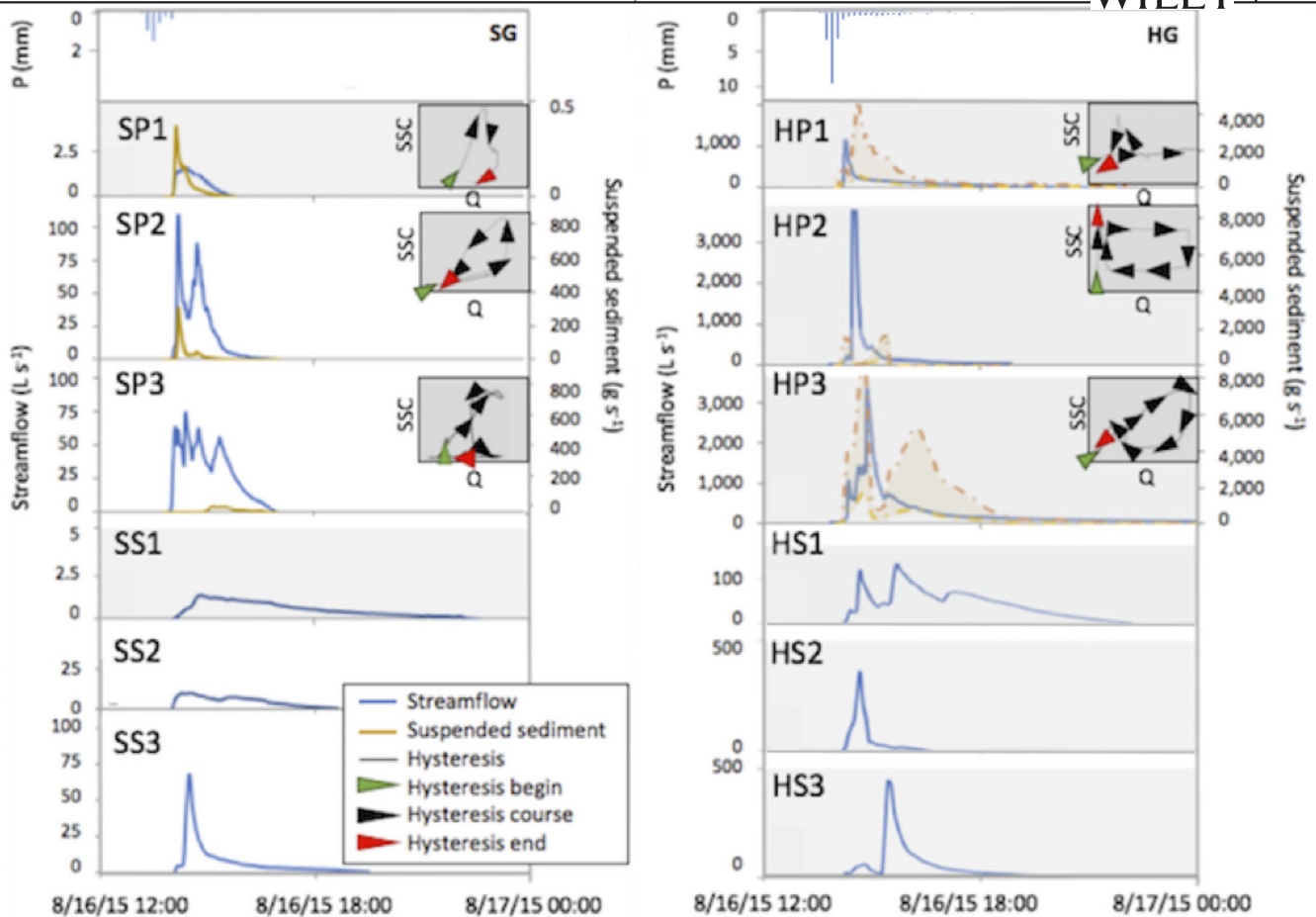
FIGURE 5 Precipitation, streamflow, and in-stream sediment responses for the rain storm on August 16th in Skin (SG; left) and Hill Gulch (HG; right). The top panel shows rainfall depth (P; mm), and subsequent panels show streamflow (Q; L s^{-1}), suspended sediment concentration (SSC; g s^{-1}), and hysteresis patterns (inset; Q vs. SSC) for each site with available data. Site names correspond to those in Figure 1 and Table 1. Upper and lower lines for SSC at Hill Gulch primary monitoring sties (i.e., HP-) represent "high" and "low" rating curve estimates, respectively. The y-axis limits are consistent across sites where possible; shaded panels indicate a much larger range of values

collection sites in Hill Gulch (HP1-c; Table 3 and Figure 4): Q was 6 mm; overtopped sediment was 0.6 Mg ha^{-1}; and the total sediment yield was 1.7 Mg ha^{-1}. Over all hillslope monitoring sites, sediment yield (Mg ha^{-1}) was higher than observed on July 8th and increased with rainfall intensity (MI$_{30-60}$; Table S2).

In-stream runoff and sediment production values within Skin Gulch were similar or slightly lower than July 8th (Table 2, Figures 3 and 7). In contrast, streamflow within Hill Gulch was orders of magnitude higher on August 16th than on July 8th with average Q of 1.6 mm (range = 0.05 to 4.3) (Figure 4), runoff ratio of 0.07 (range = 0.002 to 0.21), and peak flow of 500 L s^{-1} km^{-2} (range = 30 to 1600) (Table 2). In-stream sediment yields ranged from 0.00001 to 0.001 Mg ha^{-1} in Skin and were much higher in Hill Gulch at 0.01–0.2 Mg ha^{-1} (Figure 4 and Table 2). Across all sites, each runoff variable (i.e., Q, Q/P, and peak flow) increased with all rainfall metrics (r^2 = 0.67 to 0.89). Sediment yields also increased with all rainfall (r^2 = 0.88 to 0.95) and runoff metrics (r^2 = 0.93 to 0.98) (Table 4).

Similar to the July 8th event, most hysteretic patterns between SSC and streamflow at the primary monitoring sites during the August 16th event were clockwise, indicating in-stream sources of sediment.

The exceptions were the Hill Gulch headwater (HP1) and Skin Gulch intermediate (SP2) sites, which had predominantly counterclockwise loops, indicating the prevalence of hillslope inputs. Secondary loops were observed at most sites, indicating sediment was delivered from both in-stream sources and hillslopes (Figure 5). SDRs from hillslopes to streams were much lower in Skin (<1–30%) than in Hill Gulch (<1–3000%; Table 3). Higher hillslope-to-stream SDRs in Hill Gulch are probably due to higher rainfall intensities (Figure 4), greater runoff, and therefore greater sediment yields (Tables 2 and S2) in Hill Gulch as compared to Skin Gulch. Catchments with high hillslope-to-stream SDRs in Hill Gulch also contained a lower percent of unconfined channel length (Table 1), indicating fewer potential locations for sediment deposition between hillslopes and channels.

Average SDRs from hillslopes to streams for Hill Gulch headwater (HP1), intermediate (HP2) and outlet (HP3) were 1,000%, 80%, and 100% (Table 3), respectively, indicating much greater sediment yields from catchments than hillslopes for the headwater site (HP1). This is probably due to the high rainfall intensities and sediment yields in HP1 as compared to other parts of the watershed (Figure 4). Upstream-to-downstream SDRs in Hill Gulch ranged from 5% to

300% with the highest value for the watershed outlet (HP3; Table 3). Conversely, upstream-to-downstream SDRs decreased downstream in Skin Gulch with values of 10,000% for the intermediate Skin Gulch site (SP2) and 10% for the outlet (SP3). Similar to July 8th, hillslope-to-stream SDRs increased with the percent of a catchment that burned at high severity (Table 4).

In-stream surveys predominantly reveal deposition during the August 16th event. All cross-sections in Skin Gulch had deposition with an average of 0.1 m^2 (0.03–0.4; Table 4). Most (73%) of the cross-sections in Hill Gulch had deposition with an average of 0.3 m^2 (0.1–0.7 m^2), or 300% greater than sites in Skin Gulch for this event (Table S4 and Figures S3-S8). Cross-section-specific deposition during this event was four times higher than the July 8th event across sites in Skin Gulch, and eight times higher across sites in Hill Gulch (Table 4 and Figures S3-S8). Normalised net and absolute changes in cross-sectional area increased with the percent of a catchment that burned at high severity (Table 4).

4 | DISCUSSION

4.1 | Event magnitudes and channel responses with comparisons to other regional studies

Streamflow from commonly occurring rainfall events is generally higher post-fire (Hallema et al., 2017; Leibowitz et al., 2018; Moody & Martin, 2001a), but this effect decreases over time. Our study took place during the third-year post-fire, when runoff responses had already started to decline. Peak flows at the outlets of Skin and Hill Gulch for the July 8th event were lower than 2-year regional peak flow estimates (https://streamstats.usgs.gov/ss/). For the August 16th event, peak flow was 280 L s^{-1} km^{-2} at the outlet of Hill Gulch (HP3) which is between the 2- and 5-year peak flow estimates for this location of 111 L s^{-1} km^{-2} and 360 L s^{-1} km^{-2}, respectively. For comparison, the snowmelt runoff peak for HP3 in 2015 was 82 L s^{-1} km^{-2}. At the outlet of Skin Gulch (SP3), snowmelt runoff in 2015 exceeded the peak flow of both storms documented here at 58 L s^{-1} km^{-2}; for comparison, the 2- and 5-year regional peak flow estimates for SP3 are 83 and 238 L s^{-1} km^{-2}, respectively.

The peak flows we observed in post-fire year 3 were similar to observations within other Colorado Front Range fires (Kunze & Stednick, 2006; Moody & Martin, 2001a) and lower than those observed in post-fire years 0-1 of the High Park Fire (Brogan et al., 2017). Precipitation and streamflow were available for comparison from two watersheds (26.8 and 122.4 km^2) of the 1996 Buffalo Creek Fire for post-fire years 0–4 (Moody & Martin, 2001a) and from two watersheds (2.2 and 3.9 km^2) of the 2000 Bobcat Fire for post-fire years 0-2 (Kunze & Stednick, 2006) (Figure 6). For events with similar maximum 30-minute rainfall intensity (MI$_{30}$), peak flow during the July 8th event was slightly higher than comparable rainfall events within the Buffalo Creek Fire (post-fire years 1–4) and Bobcat Fire (post-fire year 1) (Figure 6). During the August 16th event, peak flow was similar to, or slightly higher than, comparable rainfall events
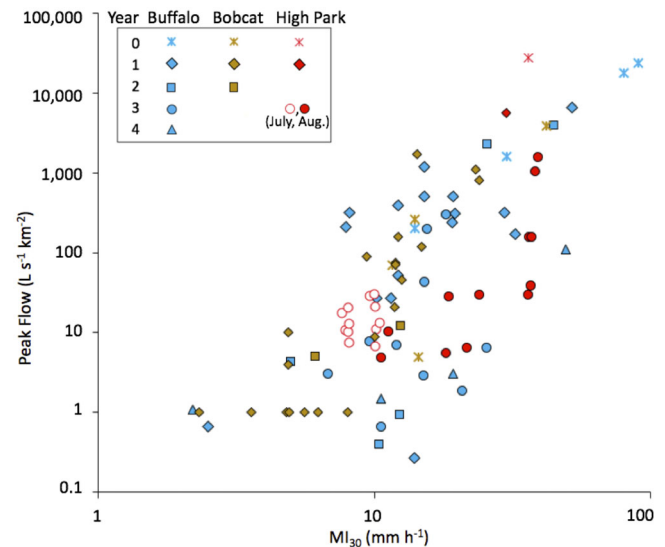
FIGURE 6 Area-normalised peak flow (L s^{-1} km^{-2}) vs. maximum 30-minute rainfall intensity (MI$_{30}$; mm hr^{-1}) by year post-fire (Year) for three fires in the Colorado Front Range: the 1996 Buffalo Creek fire (Buffalo); the 2000 Bobcat fire; and the 2012 High Park Fire. The data consist of: two watersheds each from the Buffalo Creek (26.8 and 122.4 km^2) (Moody & Martin, 2001a) and Bobcat fire (2.2 and 3.9 km^2) (Kunze & Stednick, 2006); and values for post-fire years 0–1 (15.5 km^2) (Brogan et al., 2017) and Table 1 for the High Park Fire

within the Buffalo Creek Fire (post-fire years 1–4) and Bobcat Fire post-fire years 0–2 (Figure 6).

Peak flows in the High Park Fire during post-fire years 0-1 were orders of magnitude higher than many of those observed during post-fire year 3 (Table 2). In post-fire year 0, peak flow from a 2-year storm was 28,000 L s^{-1} km^{-2} and led to widespread deposition in channels and floodplains of the lower reaches. In post-fire year 1, a long-duration mesoscale storm with a return interval of at least 200 years occurred over a week in mid-September 2013; peak flow was 5,700 L s^{-1} km^{-2} and led to extensive channel incision and migration (Brogan et al., 2017) (Figure 6 and Section S1.2). The more limited streamflow responses observed in post-fire year 3 as compared to years 0–1 could be due to differences in rainfall and vegetative regrowth; however, the patterns of responses were consistent as high intensity rainfall led to in-stream deposition and low intensity rainfall led to channel incision.

Sediment yields in this study were generally lower for in-stream sites than hillslopes, which contrasts with the general pattern observed across the western US by Moody and Martin (2009). That study found average post-fire sediment yields were higher for channels at 240 Mg ha^{-1} (range = 0.12 to 2800) than for hillslopes at 82 Mg ha^{-1} (range = 0.03 to 670). Hillslope sediment yields in our study averaged 0.24 Mg ha^{-1} (range = 0.001 to 1.7), whereas maximum in-stream sediment yields during the July 8th and August 16th event were 0.003 and 0.2 Mg ha^{-1}, respectively (Table 3). In-stream sediment yields in the Bobcat Fire, which were only reported for post-fire year 1 (compared to post-fire year 3 for our observations), were

higher at up to 0.4 and 1 Mg ha^{-1} in Bobcat (2.2 km^2) and Jug Gulch (3.9 km^2), respectively (Kunze & Stednick, 2006). Disparities in the relative magnitudes of hillslope and in-stream sediment yields may reflect the timing of observations post-fire, variable recovery times for streamflow vs. sediment responses, or legacy effects from previous rainfall events. The hillslope erosion we observed was relatively limited because our observations were collected two years after peak post-High Park Fire erosion occurred (Schmeer et al., 2018). In the first two years after the High Park Fire, deposition was common during convective storms (Brogan et al., 2017; Kampf et al., 2016), and this sediment could easily be eroded and transported during subsequent storms. Net export of sediment from streams during post-fire year 3 is supported by the SDR values >100% that we observed.

4.2 | Connectivity

4.2.1 | July 8th: Low intensity precipitation leads to low hillslope-to-stream connectivity and high upstream-to-downstream connectivity

During the July 8th event, hillslope-to-stream connectivity of runoff and sediment was low, as indicated by low hillslope erosion and low SDRs (Table 3). Upstream-to-downstream connectivity was higher but varied between watersheds (Figure 7). In-stream runoff (mm) and sediment yields (Mg ha^{-1}) generally increased with drainage area in Skin Gulch, indicating high upstream-downstream connectivity, whereas the opposite was true in Hill Gulch (Figure 7). While Q was positively correlated to P > 10 (mm) across all sites, rainfall was below the post-fire year three MI$_{60}$ thresholds of 7–10 mm hr^{-1} for watershed-scale

Q production (Wilson et al., 2018; Table 2). The runoff generated from the relatively low intensity rainfall on July 8th was probably facilitated by the high antecedent precipitation in the days prior to this storm. Wet antecedent conditions such as these contributed to substantially higher runoff in an unburned semiarid catchment (2.8 km^2) in New Mexico (Schoener & Stone, 2019) and reduced rainfall thresholds for the generation of streamflow during post-fire years 2–4 of the High Park fire (Wilson et al., 2018). Streamflow was more strongly correlated to watershed slope than to precipitation metrics for this event (Table 4), suggesting that runoff generation was localised in steeper parts of the watersheds.

Since little to no sediment entered the channel from hillslopes on July 8th, the stream had sufficient sediment transport capacity to incise stream bed sediments (Table S4 and Figure S3-S8). In-stream sources of sediment are supported by the SSC-streamflow hysteresis patterns (Figures 3 and 7) and the significant increases in cross-sectional area with increasing streamflow (Table 4). The longer-duration and widespread rainfall (Figure 4), combined with the predominantly in-stream sources of sediment, support greater upstream-downstream connectivity.

4.2.2 | August 16th: High intensity rainfall leads to high hillslope-to-stream connectivity and spatially variable upstream-to-downstream connectivity

Rainfall intensities during the August 16th event exceeded the estimated MI$_{60}$ rainfall thresholds for streamflow production of 7–10 mm hr^{-1} (Wilson et al., 2018) at all but the two headwater sites in Skin Gulch (SP1, SS1) (Figure 1 and Table 2). These two headwater
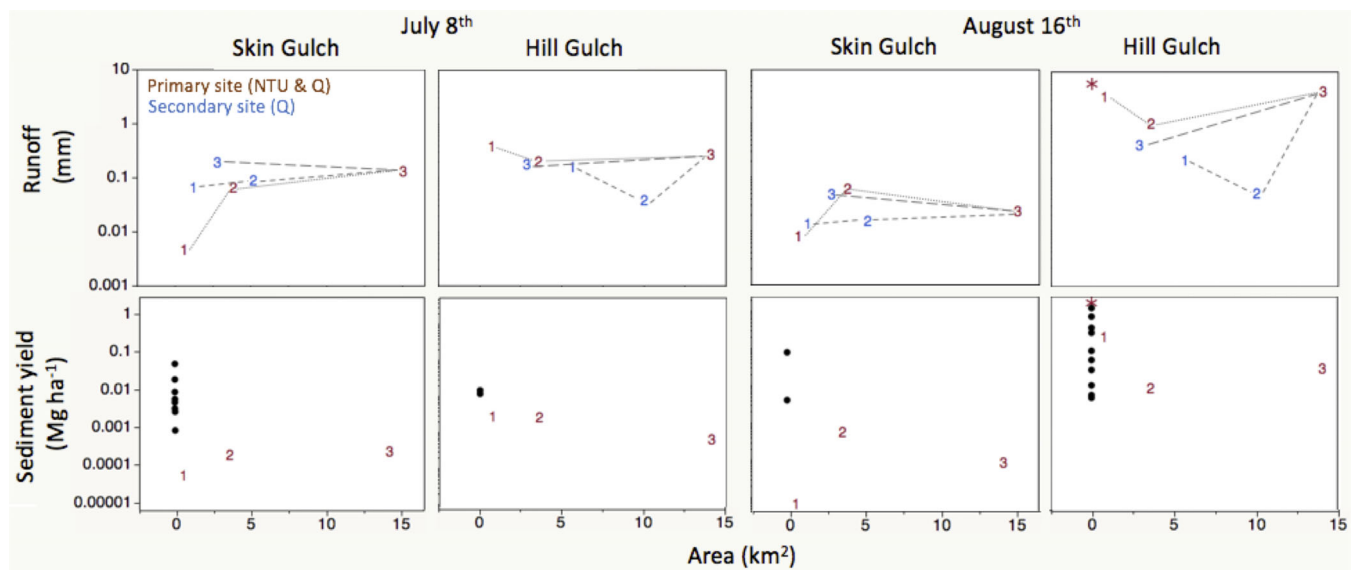
FIGURE 7 Runoff (mm) and sediment yields (Mg ha^{-1}) vs. drainage area (km^2) by rain storm (July 8th and August 16th) in Skin and Hill Gulch. The colors and numbers in the plots represent the primary (red; SP- or HP-) and secondary (blue; SS- or HS-) monitoring sites, and correspond to those in Table 1 and Figure 1. The lines between sites represent upstream (-1) to downstream (-2, -3) connectivity. The asterisk represents hillslope runoff and sediment production from HP1-c and the circles represent sediment fences

sites had the lowest runoff (mm) and sediment yields (Mg ha^{-1}) of any site (Figure 7), however production in Skin Gulch peaked just downstream at the intermediate site (SP2) (Figure 7). Despite high intensity rainfall between this site (SP2) and the watershed outlet (SP3) (Figure 4), runoff and sediment were attenuated, as indicated by decreasing upstream-to-downstream SDRs (Figure 7). In Hill Gulch, runoff (mm) and sediment yields (Mg ha^{-1}) were lowest at the intermediate sites (HP2, HS2), but increased towards the watershed outlet (HP3) (Figure 7). Production at HP3 increased with additional inputs of runoff and sediment from HS3 (Figures 1 and 7), which had 83% of its area burned at high severity (Table 1). Rainfall and high burn severity were probable controls on the production of runoff and sediment: aside from the percent of a catchment that burned at high severity, neither hillslope nor in-stream production metrics were related to any watershed attributes, whereas production uniformly increased with rainfall (Tables S2, 4).

Hillslope-to-stream sediment connectivity, as indicated by SDRs (Table 3), decreased with the percent of channel that was unconfined (Table 4), potentially due to storage of hillslope sediments in unconfined valley bottoms and near channel corridors. However, in Hill Gulch 60% of hillslope-to-stream SDRs were >100% (Table 3), indicating sediment yields were higher for in-stream sites than for the associated hillslopes. Upstream-downstream SDR was >100% at the outlet of Hill Gulch (HP3). These elevated in-stream sediment yields, which increased with all rainfall metrics and peak flow, may partially be attributed to observed stream bank erosion (Tables 4, S4 and Figures S3–S8).

Upstream-to-downstream SDRs were generally lower than hillslope-to-stream SDRs because sediment delivered to streams was deposited in-stream before reaching the watershed outlet (Tables 4, S4 and Figures S3–S8). In-stream sediment deposition (Table, S4 and Figures S3–S8) and fining (Section S1.4 and Figure S9) were greatest at the Hill Gulch headwater (HP1) and intermediate (HP2) sites, indicating decreased transport capacity. A culvert upstream of HP2 (Figure S7) may have caused water to back up, inducing deposition and reducing sediment yields. Decreased transport capacity and supply of fine sediment is supported by the downstream decline in SSC in Hill Gulch. Fine sediment deposition was lowest at the watershed outlet (HP3) likely due to convergence of streamflow from HS3 (Figure 4) and subsequent high transport capacity, as indicated by increases in the percent cobble and movement of large woody debris (Video S1, Section S1.4, and Figure S9).

4.3 | Wildfire effects on connectivity

Several results from this study suggest that the 2012 High Park fire was continuing to affect runoff and sediment responses during both the July 8th and August 16th storms. The percent of a watershed that burned at high severity was correlated with increased hillslope-to-stream SDRs and greater area-normalised cross-sectional change (Table 4). This is consistent with other studies that show increased bare soil after disturbances such as wildfire promotes hillslope erosion

(Williams et al., 2016) and connectivity of runoff and sediment from hillslopes to channels (Ortíz-Rodríquez et al., 2019). For regions with spatially variable, high intensity rainfall (Osborn & Laursen, 1973) such storms can produce localised hillslope erosion (e.g., Figure 4) and subsequent deposition of sediment within channels when the sediment delivered from hillslopes exceeds in-stream transport capacity. The relationship between high burn severity and channel change was observed for primary sites within Skin and Hill Gulch as the percent high severity burn (Figure 1 and Table 1) and channel change were highest for the headwater catchments (SP1, HP1) and generally decreased towards the watershed outlets (SP3, HP3) (Table S4 and Figures S3–S8).

The increases in connectivity after wildfire should be similar in many post-fire environments, but this study suggests that the extent of connectivity will vary with the amounts and intensity of rainfall and antecedent precipitation. In areas with high intensity convective rainfall, overland flow will produce hydrographs that rise and fall quickly; the limited spatial extent of these storms and changes in channel gradient can be expected to cause sediment deposition further downstream. In wetter regions, more sustained streamflow may occur and result in less in-stream aggradation. The spatial and temporal variations in post-fire responses warrant a nested sampling approach for the examination of runoff and sediment connectivity. Nested sampling will allow both a comparison of responses throughout a watershed, and an understanding of the processes controlling the transport of runoff and sediment into and through a stream channel network. This understanding is crucial to predicting the effect of wildfires on downstream resources of concern, and can help prioritise areas where mitigation or restoration activities can have the greatest benefit.

4.4 | Uncertainties

In the dynamic post-fire environment obtaining accurate measurements of runoff and sediment transport is extremely difficult, and the values presented here have fairly high uncertainty. Hillslope runoff measurements are affected by the accuracy of the weir equation and stage readings from cameras, which exclude any water that ponds or infiltrates inside the sediment fence (e.g., Wilson et al., 2020). Streamflow and in-stream sediment yields are affected by the accuracy of the rating curves. When streams are subject to incision and deposition, such as in a post-fire environment, the stage-streamflow relationships may vary as the cross-sectional area changes between storms. In this study, the magnitude of cross-sectional change observed did not produce noticeable offsets in the stage-streamflow rating curves leading up to the August 16th event. For this storm, rating curves had to extrapolated to obtain the highest streamflow values, as stage height exceeded observed measurements (Section S1.2). The greatest uncertainty was for the in-stream sediment yields: for the August 16th event, sediment concentrations at the highest flows were obtained from siphon samples, which generally had higher SSC than samples obtained by the ISCOs or depth-integrated samplers (Figure S2). Accurate measurement of post-fire

peak flows and sediment yields remains difficult given the short duration of most storms, difficulty of field sampling, rapid changes in cross-sectional area, and limitations of point-based samples as compared to depth-integrated samples.

5 | CONCLUSIONS

This research examined the connectivity of post-fire runoff and sediment from hillslope through watershed scales during the third summer after the 2012 High Park Fire in northcentral Colorado. We identified sources and quantified magnitudes of runoff and sediment during two rain storms with very different intensities, durations, and antecedent precipitation. The first rain storm was low intensity and long duration ($\bar{x}$ = 11 h; return interval of <1–2 years), and led to low hillslope sediment yields, limited hillslope-to-stream connectivity, and widespread channel incision because channel transport capacity exceeded hillslope sediment supply. The second storm was high intensity and short duration ($\bar{x}$ = 1 h; return interval <1–10 years), and led to: infiltration-excess overland flow, higher hillslope sediment yields with greater hillslope-to-stream sediment delivery ratios, and net aggradation within the stream channel at most sites, but not all. For this storm, sediment supply relative to transport capacity varied along the channel network: unconfined reaches of the channel network were associated with reduced delivery of sediment from hillslopes to streams, and increased streamflow and transport capacity occurred downstream from confluences. For both storms, the percent of a catchment that burned at high severity increased both hillslope-to-stream SDRs and the absolute area of cross-sectional channel change. These findings highlight the utility of nested monitoring for quantifying the connectivity of runoff and sediment in post-fire environments. The resulting data can improve our understanding of the processes that affect the spatial and temporal variability of post-fire responses. This greater understanding can improve our ability to predict downstream effects and guide post-fire mitigation and protective treatments to those areas where they can have the greatest benefit for protecting downstream receiving waters.

DATA AVAILABILITY STATEMENT

The majority of data used for this analysis are published herein or within the supplementary material. Other data available on request from the authors.

ORCID

Codie Wilson https://orcid.org/0000-0001-6296-8787
Stephanie K. Kampf https://orcid.org/0000-0001-8991-2679
Sandra Ryan https://orcid.org/0000-0002-6965-9749
Tim Covino https://orcid.org/0000-0001-7218-4927

REFERENCES

Abbott, J. T. 1970. *Geology of Precambrian rocks and isotope geochemistry of shear zones in the Big Narrows Area, Northern Front Range, Colorado*. US Geological Survey Open-File Report: 70–1. Denver, CO. p. 239.

ASTM Standard D2974-13. 2013. *Standard test methods for moisture, ash, and organic matter of peat and other organic soils*. ASTM International. Retrieved from www.astm.org

ASTM Standard D3977-97. 2013. *Standard test methods for determining sediment concentration in water samples*. ASTM International. Retrieved from www.astm.org

Beel, C. R., Orwin, J. F., & Holland, P. G. (2011). Controls on slope-to-channel fine sediment connectivity in a largely ice-free valley, Hoophorn Stream, Southern Alps, New Zealand. *Earth Surface Processes and Landforms*, 36, 981–994.

Benavides-Solorio, J. D., & MacDonald, L. H. (2005). Measurement and prediction of post-fire erosion at the hillslope scale, Colorado Front Range. *International Journal of Wildland Fire*, 14, 1–18.

Bonilla, C. A., Kroll, D. G., Norman, J. M., Yoder, D. C., Molling, C. C., Miller, P. S., ... Karthikeyan, K. G. (2006). Instrumentation for measuring runoff, sediment and chemical losses from agricultural fields. *Journal of Environmental Quality*, 35, 216–223.

Brogan, D. J., Nelson, P. A., & MacDonald, L. H. (2017). Reconstructing extreme post-wildfire floods: A comparison of convective and mesoscale events. *Earth Surface Processes and Landforms*, 42, 2505–2522.

Brogan, D. J., Nelson, P. A., & MacDonald, L. H. (2019). Spatial and temporal patterns of sediment storage and erosion following a wildfire and extreme flood. *Earth Surface Dynamics*, 7, 563–590.

Brown, L. C., & Foster, G. R. (1987). Storm erosivity using idealized intensity distributions. *Trans. ASAE*, 30(2), 379–386.

Brown, T. C., Hobbins, M. T., & Ramirez, J. A. (2008). Spatial distribution of water supply in the coterminous United States. *Journal of the American Water Resources Association*, 44(6), 1474–1487. https://doi.org/10.1111/j.1752-1688.2008.00252.x

Burned Area Emergency Response (BAER). 2012. *High park fire burned area emergency response report*. *Colorado Department of Transportation, Larimer County, NRCS, and USDA*. p. 35.

Dingman, S. I. (2002). *Physical Hydrology* (2nd ed.). Prentice-Hall Inc.

Duvert, C., Gratiot, N., Anguiano-Valencia, R., Nemery, J., Mendoza, M. E., Carlón-Allende, T., ... Esteves, M. (2011). Baseflow control on sediment flux connectivity: Insights from a nested catchment study in Central Mexico. *Catena*, 87, 129–140.

Ebel, B. A., & Martin, D. A. (2017). Meta-analysis of field-saturated hydraulic conductivity recovery following wildland fire: Applications for hydrologic model parameterization and resilience assessment. *Hydrological Processes*, 31, 3682–3696.

Emelko, M. B., Silins, U., Bladon, K. D., & Stone, M. (2011). Implications of land disturbance on drinking water treatability in a changing climate: Demonstrating the need for "source water supply and protection" strategies. *Water Research*, 45(2), 461–472.

ESRI. (2013). *ArcGIS Desktop: Release 10.3*. Environmental Systems Research Institute.

Haan, C. T., Barfield, B. J., & Hayes, J. C. (1994). *Design hydrology and sedimentology for small catchments*. Academic Press, Inc.

Hallema, D. W., Sun, G., Bladon, K., Norman, S. P., Caldwell, P. V., Liu, Y., & McNulty, S. G. (2017). Regional patterns of postwildfire streamflow response in the western United States: The importance of scale-

specific connectivity. *Hydrological Processes*, 0, 1–17. https://doi.org/10.1002/hyp.11208

Heckman, T., Cavalli, M., Cerdan, O., Foerster, S., Javaux, M., Lode, E., ... Brardinoni, F. (2018). Indices of sediment connectivity: Opportunities, challenges and limitations. *Earth-Science Reviews*, 187, 77–108.

Hewlett, J. D., & Hibbert, A. R. (1967). Factors affecting the response of small watersheds to precipitation in humid areas. In W. E. Sopper & H. W. Lull (Eds.), *Forest Hydrology, Proceedings of a National Science Foundation Advanced Science Seminar. August 29 to September 10, 1965, University Park, PA* (pp. 275–290). Pergamon Press.

Hohner, A. K., Cawley, K., Oropeza, J., Summers, R. S., & Rosario-Ortiz, F. L. (2016). Drinking water treatment response following a Colorado wildfire. *Water Research*, 105, 187–198.

Kampf, S. K., Brogan, D. J., Schmeer, S., MacDonald, L. H., & Nelson, P. A. (2016). How do geomorphic effects of rainfall vary with storm type and spatial scale in a post-fire landscape? *Geomorphology*, 273, 39–51.

Kampf, S. K., & Lefsky, M. A. (2015). Transition of dominant peak flow source from snowmelt to rainfall along the Colorado Front Range: Historical patterns, trends, and lessons from the 2013 Colorado Front Range floods. *Water Resources Research*, 52, 407–422. https://doi.org/10.1002/2015WR017784

Kilpatrick, F. A. & Cobb E.D. 1985. Measurement of discharge using tracers: U.S. Geological Survey Techniques of Water-Resources Investigations, book 3, chap. A16. p. 52.

Kunze, M. D., & Stednick, J. D. (2006). Streamflow and suspended sediment yield following the 2000 Bobcat fire, Colorado. *Hydrological Processes*, 20, 1661–1681.

Langhans, C., Nyman, P., Noske, P. J., Van der Sant, R. E., Lane, P. N. J., & Sheridan, G. J. (2017). Post-fire hillslope debris flows: Evidence of a distinct erosion process. *Geomorphology*, 295, 55–75.

Larsen, I. J., MacDonald, L. H., Brown, E., Rough, D., Welsh, M. J., Pietraszek, J. H., ... Schaffrath, K. (2009). Causes of post-fire runoff and erosion: Water repellency, cover, or soil sealing? *Soil Science Society of America Journal*, 73, 1393–1407.

Leibowitz, S. G., Wigington, P. J., Jr., Schofield, K. A., Alexander, L. C., Vanderhoof, M. K., & Golden, H. E. (2018). Connectivity of streams and wetlands to downstream waters: An integrated systems framework. *Journal of the American Water Resources Association*, 54(2), 298–322. https://doi.org/10.1111/1752-1688.12631

Lewis, J., & Eads, R. 2009. Implementation guide for turbidity threshold sampling: principles, procedures, and analysis, Gen. Tech. Rep. PSW-GTR-212, United States Department of Agriculture, Forest Service, Pacific Southwest Research Station, Albany, CA.

Lexartza-Artza, I., & Wainwright, J. (2009). Hydrological connectivity: Linking concepts with practical implications. *Catena*, 79, 146–152.

Mackay, A. K., & Taylor, M. P. (2012). Event-based water quality sampling method for application in remote rivers. *River Research and Applications*, 28, 1105–1112.

Martin, C. 2018. *Spatial and temporal variability in channel surface flow across an elevation gradient on the Colorado Front Range*. M.S. Thesis, Colorado State University. Retrieved from https://hdl.handle.net/10217/189375

Martin, D. A. (2016). At the nexus of fire, water and society. *Philosophical Transactions of the Royal Society B: Biological Sciences*, 371, 20150172. https://doi.org/10.1098/rstb.2015.0172

Moody, J. A., & Martin, D. A. (2001a). Initial hydrologic and geomorphic response following a wildfire in the Colorado Front Range. *Earth Surface Processes and Landforms*, 26, 1049–1070.

Moody, J. A., & Martin, D. A. (2001b). Post-fire, rainfall intensity-peak discharge relations for three mountainous watersheds in the western USA. *Hydrological Processes*, 15, 2981–2993.

Moody, J. A., & Martin, D. A. (2009). Synthesis of sediment yields after wildland fire in different rainfall regimes in the western United States. *International Journal of Wildland Fire*, 18, 96–115.

Moody, J. A., Shakesby, R. A., Robichaud, P. R., Cannon, S. H., & Martin, D. A. (2013). Current research issues related to post-wildfire runoff and erosion processes. *Earth-Science Reviews*, 122, 10–37.

Moreno-de Las Heras, M., Nicolau, J. M., & Merino-Martin, L. (2010). Plot-scale effects on runoff and erosion along a slope degradation gradient. *Water Resources Research*, 46, W04503. https://doi.org/10.1029/2009WR007875

Murphy, S. F., McCleskey, R. B., Martin, D. A., Writer, J. H., & Ebel, B. A. (2018). Fire, flood and drought: Extreme climate events alter flow paths and stream chemistry. *Journal of Geophysical Research: Biogeosciences*, 123, 2513–2526. https://doi.org/10.1029/2017JG004349

Nagel, D. E., Buffington, J. M., Parkes, S. L., Wenger, S., & Goode, J. R.. 2014. A landscape scale valley confinement algorithm: Delineating unconfined valley bottoms for geomorphic, aquatic, and riparian applications. Gen. Tech. Rep. RMRS- GTR-321. Fort Collins, CO: U.S. Department of Agriculture, Forest Service, Rocky Mountain Research Station. p. 42.

Nolan, K. M., & Shields R. R. 2000. *Measurement of stream discharge by wading*, U.S. Geol. Surv. Water Resources Investigation Report 00-4036, [On CD-ROM].

Ortíz-Rodríguez, A. J., Muñoz-Robles, C., & Borselli, L. (2019). Changes in connectivity and hydrological efficiency following wildland fires in Sierra Madre Oriental, Mexico. *Science of the Total Environment*, 655, 112–128.

Osborn, H. B., & Laursen, E. M. (1973). Thunderstorm runoff in southeastern Arizona. *Journal of the Hydraulics Division*, 99, 1129–1145.

Parsons, A. J., Brazier, R. E., Wainwright, J., & Powell, M. (2006). Scale relationships in hillslope runoff and erosion. *Earth Surface Processes and Landforms*, 31, 1384–1393.

Perica, S., Martin, D., Pavlovic, S., Roy, I., St. Laurent, M., Trypaluk, C., ... Bonnin, G. (2013). *NOAA Atlas 14 Volume 8 Version 2, Precipitation-Frequency Atlas of the United States, Midwestern States*. NOAA, National Weather Service.

R Core Team. 2017. *R: A language and environment for statistical computing*. R Foundation for Statistical Computing. Retrieved from http://www.R-project.org/.d

Renard, K. G., Foster, G. R., Weesies, G. A., McCool, D. K., & Yoder, D. C. (1997). Predicting soil erosion by water: A guide to conservation planning with the revised universal soil loss equation (RUSLE). In *Agriculture Handbook Number 703*. Agricultural Research Service. U.S. Department of Agriculture.

Robichaud, P. R., Jordan, P., Lewis, S. A., Wagenbrenner, J. W., Ashmun, L. E., & Brown, R. E. (2013). Post-fire mulching for runoff and erosion mitigation Part I: Effectiveness at reducing hillslope erosion rates. *Catena*, 105, 75–92.

Robichaud, P. R., Wagenbrenner, J. W., Lewis, S. A., Ashmun, L. E., Brown, R. E., & Wohlgemuth, P. M. (2013). Post-fire mulching for runoff and erosion mitigation Part II: Effectiveness in reducing runoff and sediment yields from small catchments. *Catena*, 105, 93–111.

Robinne, F., Blandon, K. D., Miller, C., Parisien, M., Mathieu, J., & Flannigan, M. D. (2018). A spatial evaluation of global wildfire-water risks to human and natural systems. *Science of the Total Environment*, 610-611, 1193–1206.

Schmeer, S. R., Kampf, S. K., MacDonald, L. H., Hewitt, J., & Wilson, C. (2018). Empirical models of annual post-fire erosion on mulched and unmulched hillslopes. *Catena*, 163, 276–287.

Schoener, G., & Stone, M. C. (2019). Impact of antecedent soil moisture on runoff from a semiarid catchment. *Journal of Hydrology*, 569, 627–636.

Sheriff, S. C., Rowan, J. S., Fenton, O., Jordan, P., Melland, A. R., Mellander, P., & hUallacháin, D. Ó. (2016). Storm event suspended sediment-discharge hysteresis and controls in Agricultural Watersheds: Implications for watershed scale sediment management. *Environmental Science & Technology*, 50, 1769–1778.

Smith, H. G., Sheridan, G. J., Lane, P. N. J., Nyman, P., & Haydon, S. (2011). Wildfire effects on water quality in forest catchments: A review with implications for water supply. *Journal of Hydrology*, *396*, 170–192.

Soil Survey Staff. 2019. Natural Resource Conservation Service, United States Department of Agriculture. Soil Survey Geographic (SSURGO) Database for Colorado. Retrieved July 15, 2019 from https://sdmdataaccess.sc.egov.usda.gov

Stone, B. 2015. *Mapping burn severity, pine beetle infestation, and their interactions at the High Park Fire*. M. S. Thesis, Colorado State University. Retrieved from http://hdl.handle.net/10217/167258

USDA-ARS (United States Department of Agriculture-Agricultural Research Service). 2019. Rainfall Intensity Summariation Tool (RIST) (Version 3.99) [computer software]. United States Department of Agriculture. Retrieved from http://www.ars.usda.gov/Research/docs.htm?docid=3251.

Wagenbrenner, J. W., MacDonald, L. H., Coates, R. N., Robichaud, P. R., & Brown, R. E. (2015). Effects of post-fire salvage logging and a skid trail treatment on ground cover, soils, and sediment production in the interior western United States. *Forest Ecology and Management, 335*, 176–193.

Wagenbrenner, J. W., MacDonald, L. H., & Rough, D. (2006). Effectiveness of three post-fire rehabilitation treatments in the Colorado Front Range. *Hydrological Processes*, *20*, 2989–3006.

Wagenbrenner, J. W., & Robichaud, P. R. (2014). Post-fire bedload sediment delivery across spatial scales in the interior western US. *Earth Surface Processes and Landforms*, *39*, 865–876.

Wainwright, J., Turnbull, L., Ibrahim, T. G., Lexartza-Artza, I., Thornton, S. F., & Brazier, R. E. (2011). Linking environmental régimes, space and time: Interpretations of structural and functional connectivity. *Geomorphology*, *126*, 387–404.

Walling, D. E. (1983). The sediment delivery problem. *Journal of Hydrology*, *65*, 209–237.

Westerling, A. L., Hidalgo, H. G., Cayan, D. R., & Sweetnam, T. W. (2006). Warming and earlier spring increase U. S. forest wildfire activity. *Science*, *313*, 940–943.

Williams, C. J., Pierson, F. B., Robichaud, P. R., Al-Hamdan, O. Z., Boll, J., & Strand, E. K. (2016). Structural and functional connectivity as a driver of hillslope erosion following disturbance. *International Journal of Wildland Fire, 25*, 306–321.

Williams, G. P. (1989). Sediment concentration versus water discharge during single hydrologic events in rivers. *Journal of Hydrology*, *111*, 89–101.

Wilson, C., Kampf, S. K., Wagenbrenner, J. W., MacDonald, L. H., & Gleason, H. (2020). Hillslope sediment fence catch efficiencies and particle sorting during post-fire rain storms. *Earth Surface Processes and Landforms*. https://doi.org/10.1002/esp.502

Wilson, C., Kampf, S. K., Wagengrenner, J. W., & MacDonald, L. H. (2018). Rainfall thresholds from plot to watershed scales. *Fire Ecology and Management*, *430*, 346–356.

Wohl, E. (2013). Migration of channel heads following wildfire in the Colorado Front Range, USA. *Earth Surface Processes and Landforms*, *38*, 1049–1053.

Wohl, E., & Scott, D. N. (2017). Transience of channel head locations following disturbance. *Earth Surface Processes and Landforms*, *42*, 1132–1139.

SUPPORTING INFORMATION

Additional supporting information may be found online in the Supporting Information section at the end of this article.